THE JOURNAL OF BIOLOGICAL CHEMISTRY
Vol. 274, No. 4, Issue of January 28, pp. 2676–2685, 2000

Printed in U.S.A.

De Novo Design of Peptides Targeted to the EF Hands of Calmodulin*

(Received for publication, August 12, 1999, and in revised form, October 19, 1999)

Matteo Villain‡, Patricia L. Jackson§¶, Michael K. Manion‡, Wen-Ji Dong§, Zhengchang Su‡, Giorgio Fassina‖, Tonny M. Johnson§, Ted T. Sakai§, N. Rama Krishna§, and J. Edwin Blalock‡

From the ‡Department of Physiology and Biophysics and §Department of Biochemistry and Molecular Genetics, Cancer Center, Schools of Medicine and Dentistry, University of Alabama at Birmingham, Birmingham, Alabama 35294 and ‖Tecnogen, 81015 Piana di Monte Verna, CE Italy

This report describes the use of the concept of inversion of hydropathy patterns to the *de novo* design of peptides targeted to a predetermined site on a protein. Eight- and 12-residue peptides were constructed with the EF hands or Ca^{2+}-coordinating sites of calmodulin as their anticipated points of interaction. These peptides, but not unrelated peptides nor those with the same amino acid composition but a scrambled sequence, interacted with the two carboxyl-terminal Ca^{2+}-binding sites of calmodulin as well as the EF hands of troponin C. The interactions resulted in a conformational change whereby the 8-mer peptide-calmodulin complex could activate phosphodiesterase in the absence of Ca^{2+}. In contrast, the 12-mer peptide-calmodulin complex did not activate phosphodiesterase but rather inhibited activation by Ca^{2+}. This inhibition could be overcome by high levels of Ca^{2+}. Thus, it would appear that the aforementioned concept can be used to make peptide agonists and antagonists that are targeted to predetermined sites on proteins such as calmodulin.

Accumulating evidence suggests that a simple binary code of polar and nonpolar amino acids arranged in the appropriate order is sufficient to build helical bundle structures and artificial peptides with rudimentary function (for review see Ref. 1). Therefore, only the sequence location, not the identity, of the polar and nonpolar amino acids must be explicitly specified for the formation of a stable helical structure or biologically active peptide. Such binary coding has been successfully employed to produce biologically active analogs of corticotrophin and growth hormone-releasing hormone (2, 3), to design proteins that fold into compact α-helical bundles (4), and to develop computer programs that simulate or predict some aspects of protein folding (5). Considering that 20 different amino acids are encompassed by the binary code, one would expect a marked degree of sequence degeneracy for a given shape, since any one of a number of specific polar or nonpolar amino acids could occupy a given position in the sequence. Indeed, experimental evidence has confirmed that gross shape is degenerate with regard to sequence in that any number of different primary amino acid sequences with the same binary code can fold into compact α-helical structures (4).

More recent studies have shown that, unlike simple helical structures, a five-letter amino acid alphabet is minimally required to build a well ordered, β-sheet containing protein architecture (6). In this particular instance, a small β-sheet protein, the SH3 domain, could be constructed with 95% of the residues being Ile, Lys, Glu, Ala, and Gly. Interestingly, the pattern of hydropathy of the wild type SH3 domain was largely maintained in the two sequence-simplified structures.[1] This would seem once again to point to the importance of the pattern of hydropathy in building more complex structures as well as simple helical ones.

If, as described above, the gross architecture of a peptide or protein is in part determined by its pattern of hydropathy, then exactly inverting a particular pattern or code may result in a second peptide or protein with a complementary surface contour to the first since the hydrophobic effect is involved yet in reversed orientation (for review see Ref. 1). Inversion of the hydropathic pattern of one sequence relative to another can be achieved by computer programs designed for this task (7–9) or by simple reliance on an interesting characteristic of the genetic code (10). In the later instance, since A and U are complementary and in the second codon position specify hydrophilic and hydrophobic R groups, respectively, and considering that second base G and C generally encode slightly hydrophilic R groups, amino acid sequences deciphered from noncoding strands of DNA will have exactly inverted patterns of hydropathy relative to those of coding strands (for review see Ref. 1).

Such peptides specified by complementary nucleotide sequences (11) or designed by simply inverting the hydropathic pattern (8) are termed complementary peptides and have characteristics suggestive of complementary structure. For instance, we and many others (for review see Refs. 1 and 12) have shown that in almost 40 different systems complementary peptides bind one another with specificity and moderate affinity. Additional evidence of complementary structure includes the following: the ability to locate the interactive sites of ligands and receptors by identification of complementary sequences (13–17); to generate interacting pairs of monoclonal idiotypic and anti-idiotypic antibodies with complementary combining sites by immunization with pairs of complementary peptides (18–27); to produce antibodies to receptor-binding sites by immunization with complementary peptides for the receptor's ligand (11, 18, 27–34). Most recently, a novel hormone receptor was cloned, and its binding site was localized using

* This work was supported in part by National Institutes of Health Grant MH52527, NCI Grant CA13148 from the National Institutes of Health, and National Science Foundation Grant MCB96. The costs of publication of this article were defrayed in part by the payment of page charges. This article must therefore be hereby marked "*advertisement*" in accordance with 18 U.S.C. Section 1734 solely to indicate this fact.

The atomic coordinates and structure factors (code 1CMG) have been deposited in the Protein Data Bank, Research Collaboratory for Structural Bioinformatics, Rutgers University, New Brunswick, NJ (http://www.rcsb.org/).

¶ Current address: Dept. of Chemistry, University of Alabama at Birmingham, Birmingham, AL 35294.

** To whom correspondence should be addressed. Tel.: 205-934-6439; Fax: 205-934-1446; E-mail: Blalock@physiology.uab.edu.

[1] M. Villain and J. E. Blalock, unpublished observations.

this principle (17). Not unexpectedly, the aforementioned degeneracy that is observed for the relationship between sequence and structure applies to the complementary sequence since the same codes are operative. Thus a number of complementary peptides that are properly patterned are predicted to bind the appropriate target sequence. This has been previously observed (35–37).

The above results suggested that one could specifically target a complementary peptide to interact with a particular site(s) on a given protein. This was initially tested with an eight-residue complementary peptide (termed calcium-like peptide, CALP1) designed to interact with an EF hand motif based on the primordial Ca^{2+}-binding site of the troponin C superfamily (38). Micromolar concentrations of CALP1 together with CaM,[2] but neither CALP1 nor CaM alone, were found to activate phosphodiesterase in the absence of Ca^{2+}. This demonstrated that the combination of CALP1 and CaM functioned similarly to a combination of Ca^{2+} and CaM. These results implied but did not prove that CALP1 directly interacted with CaM. Thus in the present studies we have sought evidence for direct binding of CALP1 to CaM, and we tested whether this occurs at or near the EF hands of CaM. Also, as a consequence of the CALP1 design being based on the primordial EF hand motif (38, 39), the hydropathic profile of CALP1 is not perfectly inverted relative to the EF hand motifs of CaM. In the present study, we have designed a complementary peptide to invert more perfectly the pattern of hydropathy and to extend the sequence length to determine the role of these two factors on the interaction with CaM. Specifically, we synthesized a 12-mer peptide (CALP2; Table I) with an optimized and extended inverted hydropathic profile to EF hand motif 4 of human CaM using AMINOMAT® (Tecnogen, Italy) (40), a computer program able to determine the optimal complementary peptide sequence to a target. In order to distinguish if any increased affinity was due to the optimal hydropathic pattern or to the increased length or both, we also synthesized CALP3, which represents the first eight residues of CALP2, and CALP4, a 12-mer peptide identical to CALP1 in the first eight residues and CALP2 in the last four (Table I). We tested the binding characteristics of these peptides for CaM using three different approaches as follows: inhibition of complex formation between CaM and the EF hand-binding dye, Stains-all; changes in the emission spectra of dansylated CaM to monitor conformational changes; and real time measurement of the interaction with a biosensor based on surface plasmon resonance detection. We also characterized certain of the interactions with nuclear magnetic resonance spectroscopy and tested for CaM activation with a CaM-stimulated phosphodiesterase (PDE) assay. Finally, we tested the generality of the interaction by assessing the ability of CALP2 and -3 to bind the EF hands of another Ca^{2+}-binding protein, troponin C.

TABLE I
CALP series and hydropathy plots

Peptide names	Sequences	Hydropathy plot
EF hand loop 4	DIDGDGQVNYEE*	■
CALP1	VAITVLVK	○
CALP2	VKFGVGFKVMVF	▲
CALP3	VKFGVGFK	
CALP4	VAITVLVKVMVF	
SCRAMBLE	VVKFKFGMVFGV	

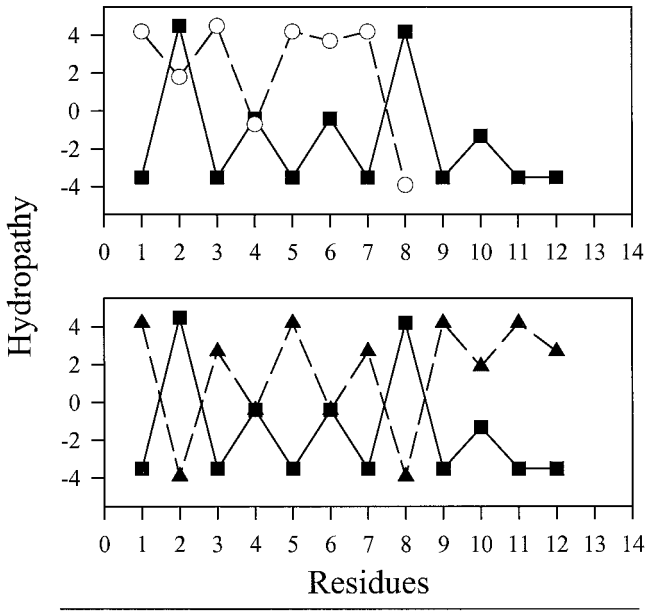

* All peptides were synthesized as amino-terminal free amine and carboxyl-terminal free carboxylic acid.

EXPERIMENTAL PROCEDURES

Precautions to Eliminate Ca^{2+} Contamination—In all the experiments, buffers were treated with the chelating resin Chelex 100. Stock solution of the peptides were checked for Ca^{2+} contamination by atomic absorption. Levels were always below 2 μM Ca^{2+}/mM CALP. Thus, Ca^{2+} contamination was at most 200 nM and was usually 2–20 nM. These levels are below those required to affect any of the assays.

Reagents—Preloaded polyethylene glycol graft polystyrene, *O*-pentafluorophenyl ester amino acid, and 1-hydroxy-7-azabenzotriazole were purchased from Perspective Biosystems (Framingham, MA). High purity CaM from bovine brain and biotin-labeled calmodulin were purchased from Calbiochem. Its purity was checked by SDS-polyacrylamide gel electrophoresis and the identity verified by electrospray ionization-mass spectroscopy (University of Alabama at Birmingham Core Facility). Neutravidin was from Pierce. D-CaM, PDE, MOPS, Chelex 100, and Stains-all were from Sigma. *N,N*-Dimethylformamide, DCM, and acetonitrile were purchased from Mallinckrodt (Paris, KY). Mant-cGMP was from Molecular Probes (Eugene, OR). All other reagents were high purity grade obtained from Fisher or Sigma.

Design of the Hydropathically Complementary Peptides—Selection of the complementary peptide targeted to CaM EF hand 4 motif was carried out as described previously (40) using the computer program AMINOMAT® (Tecnogen ScpA, Italy), with an averaging window $r = 9$, a range of inverted hydropathy of 0.8 and considering also the eight amino acids of the flanking regions. The program generated 1,417,176 possible sequences, and we chose the one with the lowest Q value (0.0068). This process resulted in a 12-residue peptide defined CALP2. CALP3 was generated by eliminating the four carboxyl-terminal amino acids of CALP2. CALP4 is a chimeric sequence carrying the eight amino acids of CALP1 with the addition at the carboxyl terminus of the four amino acids from the corresponding region of CALP2 (Table I).

A scrambled version of CALP2 and peptides with sequences not related to the CALP series were used as negative controls.

Peptide Synthesis—All the peptides were synthesized in our laboratory using continuous flow solid phase peptide synthesis with Fmoc (*N*-(9-fluorenyl)methoxycarbonyl) chemistry, on a PerSeptive Biosystems 9050 Peptide synthesizer. Pre-activated *O*-pentafluorophenyl ester amino acids with 1-hydroxy-7-azabenzotriazole and preloaded polyethylene glycol graft polystyrene resin was used. All the peptides were purified by preparative RP-HPLC. The purity of the product was checked by analytical RP-HPLC. The identity of the peptides was con-

[2] The abbreviations used are: CaM, calmodulin; D-CaM, 5-dimethylaminonaphthalene-1-sulfonyl-calmodulin; DCM, methylene chloride; Mant-cGMP, methylanthraniloyl cyclic GMP; MOPS, 3-(*N*-morpholine)propanesulfonic acid; PDE, 3′:5′-cyclic nucleotide 5′-nucleotidohydrolase activator-deficient from bovine brain; RP-HPLC, reverse phase-high performance liquid chromatography; Stains-all, 1-ethyl-2-[3-(ethylnaphtho[1,2-*d*]thiazolin-2-ylidene)-2-methylpropenyl]naphtho-[1,2-*d*]thiazolium bromide; TRC1, tryptic digested CaM fragment 1 (Ala_1-Arg_{74}); TRC2, tryptic digested CaM fragment 2 (Asp_{78}-Lys_{148}); TnC, slow muscle troponin C; Mas7, Mastoparan 7.

firmed by time of flight matrix-assisted laser desorption ionization mass spectrometry (University of Alabama at Birmingham Core Facility).

Inhibition of the CaM·Stains-all Complex—CaM was suspended in water (300 μM final concentration) and aliquoted. All the peptides were suspended in a 3.3 mM MOPS solution, pH 7.2. Stains-all dye (60 μM) in ethyl glycerol was prepared fresh before each experiment, starting from a stock solution of 500 μM. All experiments were conducted using final concentrations of 1 μM CaM and 20 μM dye. Plastic tubes and the cuvette were washed with EGTA (0.2 M) and rinsed with Chelex water to remove any traces of Ca^{2+}. For the assay 1.4 μl of CaM and different quantities of the peptides were added to 3.3 mM MOPS buffer to reach a final volume of 350 μl. The solutions were incubated at room temperature for 15 min. Ten minutes before reading, 150 μl of the dye solution was added and gently mixed. The spectra of the Stains-all·CaM complexes were recorded on a Shimadzu UV160 spectrophotometer between 400 and 700 nm. Data are presented as $(A_{[ligand]}/A_{[0]} \times 100)$ at 639 nm.

D-CaM Fluorescence Measurement—D-CaM was solubilized in buffer containing 20 mM Tris-HCl, 250 mM NaCl, 5 mM $MgCl_2$, pH 8.0. Measurements were done in duplicate on a PTI fluorescence instrument equipped with a Delta Scan™ dual monochrometer illuminator (South Brunswick, NJ) with a fixed excitation wavelength of 340 nm and scanning the emission between 400 and 600 nm. EGTA (0.5 mM final concentration) was added to the D-CaM (200 nM) solution to reverse any Ca^{2+} contamination. Increasing amounts of the peptides or Ca^{2+} were added to the solution, and the increase in emission at 494 nm was measured. Intensity data were corrected for dilution. The data are presented as $(Emission_{[ligand]}/Emission_{[0]}) \times 100$ at 490 nm.

Surface Plasmon Resonance Detection Studies—Direct measure of the affinities of the peptides for CaM were obtained using a surface plasmon resonance detector (IAsys, Affinity Sensor, Cambridge, UK). A carboxymethylated dextran cuvette was prepared immobilizing Neutravidin using an NHS/EDC activation procedure according to the manufacturer's protocols (IAsys protocol 1.1) This was followed by the attachment of biotin-labeled CaM to the Neutravidin on the cuvette. Binding buffer was 20 mM MOPS, 150 mM NaCl, pH 7.4, containing 0.05% Tween 20 treated with Chelex 100. K_d values were calculated using the software FASTfit, supplied by the manufacturers for the analysis of the binding curves. For the association, the curves were fitted to a single rate constant. For the dissociation we also used a single rate constant.

Fluorescent Troponin C—The rabbit slow muscle troponin C mutants (C84S/Y111W, C84/R147W, and C84S/Y111W/R147W) were a gift of Dr. Herbert Cheung, and their preparation and characteristics are discussed elsewhere.[3] Steady state fluorescence for peptide-protein interaction were conducted using a ISS PC1 photo-counting fluorometer using a 0.1-mm slit. Protein was solubilized at 1 μM in 50 mM MOPS, 100 mM KCl, 50 μM EDTA, pH 7.2. Peptides were solubilized at a 3 mM stock concentration in this protein containing solution. By using 295 nm as the excitation wavelength, we measured the emission spectra between 300 and 400 nm with increasing concentration of the peptides. Spectra were recorded 5 min after addition of the peptide stocks. Acrylamide quenching of CALP2·TnC complex (75 and 1 μM, respectively) and of TnC (1 μM) were conducted in the same buffer, by the addition of aliquots of an 8 M acrylamide solution with λ_{ex} = 295 nm and λ_{em} at the peak of the emission spectrum. In the range of acrylamide concentrations used (0–400 mM), we observed a linear relationship between tryptophan emission decay and quencher concentration. The quenching data were fitted to a modified Stern-Volmer equation, $F_0/F = (1 + K_{SV}[Q])$; where F_0 and F are the fluorescence intensities in the absence of and presence of quencher, respectively; $[Q]$ is the molar quencher concentration; and K_{SV} is the Stern-Volmer dynamic quenching constant.

Time-resolved fluorescence measurements were conducted as previously reported (42). Transient kinetic measurements were performed on a Hi-Tech Scientific PQ/SF-53 stopped-flow spectrometer equipped as described (43). In a typical binding experiment, one syringe contained 10 μM C84S/R147W TnC or C84S/R147W TnC together with 50 μM CALP2 in 30 mM MOPS, 100 mM KCl, and 50 μM EGTA, pH 7.2. The protein was dialyzed against Chelex 100 resin before use. The other syringe contained 10 mM Ca^{2+} in the same buffer.

Circular Dichroism—CD studies were conducted on a 62 DS VCD spectrometer AVIV (Lakewood, NJ) using a 0.01-cm quartz cuvette, with a scanning range of 195–310 nm, a time constant of 2 s, and a scanning rate of 0.5 nm/s. The buffer used was 20 mM phosphate, pH 7.0

[3] W. J. Dong, J. M. Robinson, J. Xing, P. K. Umeda, and H. C. Cheung, submitted for publication.

CaM-stimulated Phosphodiesterase (PDE) Assay—Measurements were obtained using a continuous fluorimetric assay based on Mant-cGMP. Mant-cGMP, a fluorescent derivative of cGMP, shows maximal fluorescence emission at 450 nm. Hydrolysis of Mant-cGMP by PDE in the presence of CaM and Ca^{2+} causes a decrease in the emission spectra of the compound. The enzymatic reaction can be followed in real time using 280 nm as excitation wavelength and monitoring the emitted light at 450 nm. Experiments were conducted using an excess of the substrate at fixed concentrations of CaM and PDE with constant mixing. By using these conditions the V_{max} of the reaction can be calculated by the slope of the rectilinear part of the enzymatic reaction curve. Mant-cGMP was dissolved in MeOH (1.6 mM) and kept on ice. The reaction was conducted in 0.01 M MOPS, 0.09 M KCl, 5 mM $MgCl_2$, 0.1 mM EGTA, pH 7, at 37 ± 2 °C. Mant-cGMP was diluted in the reaction buffer (8 μM final concentration) with CaM (5 nM) and the different peptides or free Ca^{2+}. The system was equilibrated for 5 min. The reaction was followed using a PTI fluorescence instrument. The rate of the reaction was calculated with a linear regression of 150 data points after addition of PDE. Excitation wavelength was 280 nm, and emitted light was monitored at 450 nm, collecting 30 data points/min. The reaction was started by addition of PDE (0.05 units/ml). For Fig. 10, the percent inhibition was calculated using the formula: $100 - ((V_{max(pep)} - V_{max(no\ Cam)})/(V_{max(no\ peptide)} - V_{max(no\ Cam)})\cdot 100)$, where $V_{max(pep)}$ is the rate of degradation of cGMP for a given Ca^{2+} concentration in presence of the peptides, $V_{max(no\ peptide)}$ is the rate of degradation for the same Ca^{2+} concentration without the peptides, and $V_{max(no\ CaM)}$ is the basal rate without CaM, defined as the basal activity of PDE.

Production of ^{15}N CaM and ^{15}N TRC1 and TRC2—Escherichia coli strain BL21 (DE3) harboring plasmid pRK7a for *Drosophila melanogaster* CaM was obtained from Dr. K. Beckingham (Rice University). Unlabeled CaM was expressed in cells grown in Terrific Broth, and ^{15}N-labeled CaM was purified from cells grown in M9 medium using $^{15}NH_4Cl$ as the sole nitrogen source. CaM (labeled and unlabeled) was purified by repeated chromatography on phenyl-Sepharose CL4B followed by ion exchange chromatography on DEAE-cellulose using a linear gradient (0–0.5 M) of sodium chloride in 0.05 M sodium phosphate, pH 5.7. Under these conditions, CaM is obtained as a single peak, eluting at ~0.35 M NaCl. ^{15}N-Labeled CaM tryptic fragments, TRC1 (amino-terminal domain) and TRC2 (carboxyl-terminal domain), were prepared as described previously (44, 45) except the purification of the two fragments was done by RP-HPLC on a Waters Delta Pack C18 300 A (300 × 39 mm inner diameter) column. The fragment identity was check by time of flight matrix-assisted laser desorption ionization mass spectrometry. NMR chemicals shift were consistent with the literature (46).

NMR Experiments—Apocalmodulin samples were prepared by dissolving the sample in 3 ml of water and dialyzed against 2 changes of 1 M EDTA, 1 mM urea, pH 7.8, (2 times) followed by 0.5 M KCl (2 times), 0.25 M KCl (2 times), and deionized, distilled water (3 times). NMR samples were prepared by dissolving the protein sample in either 100% D_2O (Cambridge Isotopes, MA) or 90% H_2O, 10% D_2O. The pH was adjusted using 0.1 mM DCl or 0.1 mM NaOD solutions. Concentrated peptide sample (2.0 mM CALP1 or 4.0 mM CALP3) solutions were prepared, the pH was adjusted and then titrated into the protein samples.

One-dimensional ^{1}H NMR spectra were acquired using a 12 ppm spectral width and presaturation of the HOD resonance. These spectra were acquired on either a Bruker WH400 or a Bruker AM600 instrument. The spectra were processing by Felix (MSI, San Diego, CA).

Two-dimensional ^{1}H-^{15}N HSQC (47) data were acquired on the Bruker AM600 instrument. The spectra were acquired with 12 ppm spectral width, 2048 complex t_2 points, and 512 t_1 points. All measurements were made at 298 K. Spectra were processed using Felix 95.0 (MSI, San Diego, CA), by zero filling to 2 by 2K data sets. Solvent suppression and first point correction were used for each spectra. A 45° shifted sinebell apodization function was applied in each dimension.

RESULTS

Surface Plasmon Resonance Detection—By using a biosensor based on surface plasmon resonance detection, we were able to measure the real time interaction of CALP1 and CALP2 with CaM (Fig. 1). This binding was specific in that free CaM (25 μM) in the binding buffer completely inhibited the interaction (data not shown). When the binding curves were analyzed with the computer program Fast-Fit, using a first order kinetic equation, CALP1 and CALP2 were found to have dissociation con-

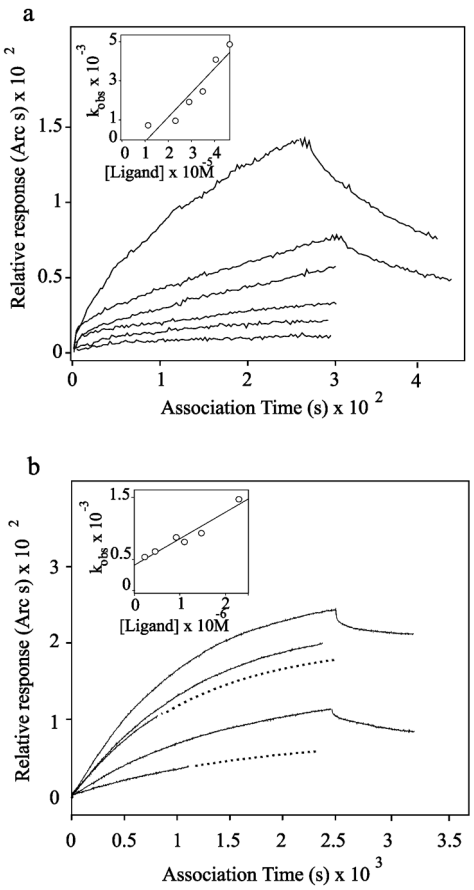

FIG. 1. **Surface plasmon resonance detection of CALP1 and CALP2 binding to CaM.** *a*, CALP1 concentrations were the *top* to the *bottom* are as follows: 41, 35.5, 29.5, 23.5, 17.5, and 11.5 μM. The calculated kinetic k_a from linear regression of the k_{obs} for each given concentration (*inset*) was 125 ± 21.7 M^{-1} s^{-1} (correlation coefficient = 0.944576). The k_d was calculated from the average of 4 dissociation experiments and was 0.011 ± 0.0035 s^{-1}. The equilibrium dissociation constant calculated as k_d/k_a was 8.8 ± 3.1 × 10^{-5} M. The K_d was also estimated using the extent of binding for each concentration and was 13.1 ± 4.5 × 10^{-5} M with a B_{max} of 451.3 Arc seconds *b*, CALP2 concentrations from the *top* to the *bottom* are as follows: 1.47, 1.11, 0.98, 0.45, and 0.36 μM. The calculated kinetic k_a (see above) was 428.13 ± 55.1208 M^{-1} s^{-1}, and the k_d was 0.0034 ± 0.00025 s^{-1} (average of 6 experiments). The K_d from the ratio of kinetic constants was estimated to be 7.9 ± 1.1 × 10^{-6} M. The K_d from the total extent was 5.2 ± 2.1 × 10^{-6} M with a B_{max} of 442.228 Arc s. The increase in affinity in CALP2 is due both to a faster k_a (~4 time) and to a slower k_d (~3 times). The absence of nonspecific binding to the resin in the concentrations used was established using a cuvette blocked with ethanolamine or derivatized with Neutravidin alone.

stant (K_d) for CaM of 88 and 7.9 μM, respectively (Fig. 1). Thus, optimizing the pattern of inverted hydropathy and increasing the complementary peptide length from 8 to 12 residues resulted in a 11-fold increase in affinity.

CALP Does Not Structurally Resemble a Common CaM-binding Motif—The binding that was observed by surface plasmon resonance detection could be due to CALP interaction with the EF hands of CaM or its hydrophobic core or both. Based on the following, it is unlikely that CALP is simply a binding peptide for the hydrophobic pocket of CaM. First, our CALP peptides don't match any of the Block consensus patterns for CaM-binding motifs (48, 49). Second, CaM-binding peptides show a high helical structural propensity. In contrast, the CD spectra for all of the CALP peptides are consistent with a β-turn (data not shown). In addition, the experimental data that follow clearly demonstrate an EF hand interaction.

Inhibition of Stains-all-Calmodulin Complex Formation—To establish experimentally that CALP bound the EF hands of CaM, we used the cationic carbocyanine dye, Stains-all, which is one of the most sensitive and useful probes for studying the calcium-binding sites of proteins such as CaM (50). This dye has been shown to bind to Ca^{2+}-binding sites or EF hand motifs and to generate characteristic spectral changes. One of the important features of Stains-all binding is the ability of Ca^{2+} to displace the dye from its binding site. Thus Stains-all binding was used to test whether the CALP peptides were interacting with the Ca^{2+}-binding sites of CaM. Fig. 2 shows that as expected Ca^{2+} can inhibit the interaction of the dye with CaM with a 50% inhibitory concentration (IC_{50}) of 2 to 3 μM. Interestingly, both CALP1 and CALP2, but not a scrambled version of CALP2, were able to block Stains-all·CaM complex formation (IC_{50} of 125 and 9 μM, respectively) (Fig. 2). Once again CALP2 had a 14-fold higher affinity than CALP1. Perhaps more importantly these results strongly suggest that the complementary peptides were interacting with the sites to which they were targeted.

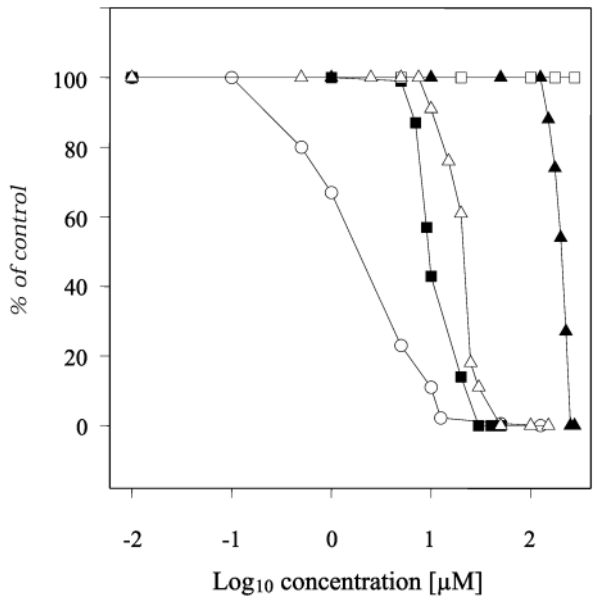

FIG. 2. **Ca^{2+} and CALP inhibition of Stains-all·CaM complex formation.** Ca^{2+} (○), CALP2 (■), CALP4 (△), and CALP1 (▲) inhibited the *J* band characteristic of the Stains-all·CaM complex, whereas the scrambled version of CALP2 (□) and other unrelated peptides (data not presented) are not active in the concentration range tested.

Conformational Changes in CaM—When Ca^{2+} binds to CaM, the protein undergoes a major change in conformation that can be monitored by a shift in the emission spectrum of dansylated CaM from a maximum at 530 to 494 nm (51) Fig. 3 shows that, like Ca^{2+}, the CALP peptides, but not control peptides, were able to induce the expected change in the emission spectrum of dansylated CaM. EGTA was added at the end of the titrations to ensure the effects were not due to Ca^{2+} contamination. EGTA addition (0.5 mM) at the end of the Ca^{2+} titration reversed the spectrum to a maximum at 530 nM. In contrast, the chelating agent caused no change in the spectra of the CALP peptides complexed with CaM (Fig. 3). Thus Ca^{2+} contamination was not responsible for the spectral changes caused by the CALP peptides. This is also in marked contrast to a typical CaM-binding compound, Mastoparan (Mas) 7, which is an amphipathic basic peptide that doesn't bind apoCaM, but interacts with the hydrophobic core of CaM after the four EF hands are occupied by Ca^{2+} (Fig. 3). This interaction causes an additional change in conformation that leads to a further increase in the emission of dansylated CaM at 494 nM (52, 53) that is completely reversible by the addition of EGTA (Fig. 3).

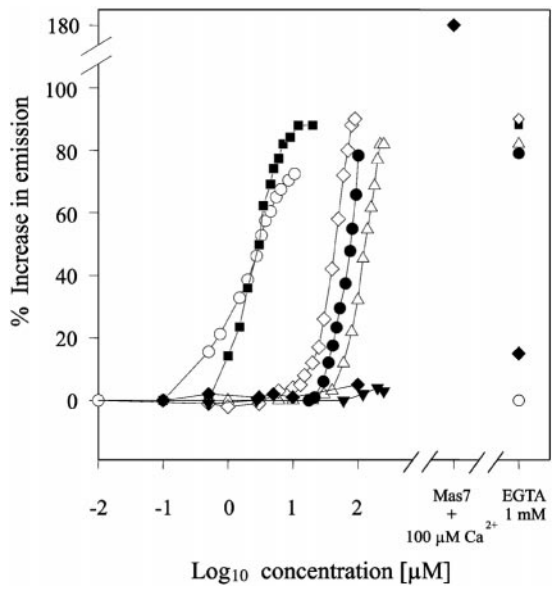

FIG. 3. **Ca^{2+}- and CALP-induced spectral changes in D-CaM.** Ca^{2+} (○), CALP2 (■), CALP1 (△), CALP3 (●), and CALP4 (◇) induced an increase in D-CaM emission at 494 nm, whereas the scrambled version (▼) of CALP2, Mastoporan 7 (♦), and other unrelated peptides did not. At the end of the titration, in the case of Ca^{2+}, addition of 1 mM EGTA reversed the emission maximum to 520 nm. Mastoporan 7 with 100 μM calcium caused an increased emission that was also reversed by EGTA. Reversion of the emission maximum to 520 nm does not occur for any of the CALP series in the presence of EGTA.

The dansylated CaM system, because of its sensitivity, was also used to evaluate the relative contribution of optimal inversion of the pattern of hydropathy and complementary peptide length on the affinity for CaM. In this assay system (Fig. 3), CALP2 had an affinity (2.4 μM) that approached that of Ca^{2+} (2.2 μM) and was 50 times higher than CALP1 (120 μM). CALP3 which represents the first eight amino acids of CALP2 and is equal in length to CALP1 was about 2-fold (66 μM) more active than CALP1. CALP4 which is the same length as CALP2 and is composed of CALP1 of four additional amino acids from the carboxyl-terminal region of CALP2 was 2.5 times (48 μM) more active than CALP1. Thus, although optimizing hydropathy or increasing length can improve the affinity, the combination of the two leads to an exponential increase.

Interaction with TnC—In order to test for the generality of CALP binding to EF hands as well as to evaluate interaction with a Ca^{2+}-binding protein that lacks a hydrophobic core, we studied the interaction of the peptides with TnC. Tyr-111 and Arg-147 of smooth muscle troponin C, corresponding to position 7 of EF hand motif III and IV, respectively, were mutated to generate either single tryptophan mutants (C84S/Y111W/TnC and C84S/R147W TnC) or double tryptophan mutants (C84S/Y111W/R147W TnC) (42).[3] One characteristic of these mutants, as seen also with similar mutants of CaM (54–56), is a quenching effect in the presence of Ca^{2+}. In the single tryptophan mutants, this is most likely due to a change in the environment of the tryptophan due to the conformational change induced by binding Ca^{2+}. In the double tryptophan mutant, Ca^{2+} co-ordination by the adjacent EF hands III and IV, results in a reduced distance between the two tryptophans leading to fluorescence self-quenching.[3] We used this system to test for an interaction of CALP with the EF hands of TnC, observing different effects with CALP2 and CALP3.

Interaction of CALP2 with C84S/Y111W/R147W TnC resulted in a strong increase (>50%) in the tryptophan emission (Fig. 4*a*) and a shift in the maximal emission from 347 to 337 nm. The concentration of CALP2 resulting in half-maximal effect is 33 μM. Neither scrambled CALP2 nor Mas7 had a significant effect on the tryptophan emission (Fig. 4*a*). Binding of Ca^{2+} to this TnC mutant causes the opposite effect, that is a quenching of the tryptophan emission.[3] CALP2 had no effect on the emission of free tryptophan (2 μM), indicating that the effect of this peptide on the emission from the TnC mutant is not due to a change in the viscosity of the solution. The same effect of CALP2 was seen when complexed with the single tryptophan mutants, although the increase in emission was lower (approximately 18% for C84S/Y111W TnC and 25% for C84S/R147W TnC) (data not shown).

Stop flow analysis was done with C84S/R147W TnC to determine the kinetics of quenching due to binding of Ca^{2+} either in the absence (Fig. 4*b*) or presence (Fig. 4*c*) of CALP2. Single exponential fitting of the association curves at saturating concentrations of Ca^{2+} gave a decay rate constant (k_1) for TnC alone of 284 s^{-1}, and for the TnC·peptide complex this was 0.38 s^{-1}. The approximately 1,000-fold slower kinetics for this quenching in the presence of the peptide indicates that CALP2 is binding in the same region, and thus competing with Ca^{2+}, analogous to the results from the Stains-all experiments. The slow dissociation of the peptide from such a site, as shown also with surface plasmon resonance detection, is the rate-limiting step for the binding of Ca^{2+} resulting in the slower kinetics.

To verify further that the effect seen with CALP2 is due to the direct interaction of the peptide with the EF hands of C84S/Y111W/R147W TnC, we measured the fluorescence parameters in the presence of a quenching agent (acrylamide, Table II). The complex of CALP2 with C84S/Y111W/R147W TnC exhibited a decrease in quenching constant (k_q) as well as an increase in the fluorescence lifetime ($<\tau>$) indicating that the tryptophan residues are buried in a more hydrophobic environment. Based on a model of the double tryptophan mutant TnC, this hydrophobic environment results from a direct binding of the peptide to the EF hands involved.

CALP3 had the opposite effect on the tryptophan emission of the double tryptophan mutant TnC, causing an 18% decrease with an IC_{50} around 400 μM (Fig. 4*d*). This is similar to the effect seen with Ca^{2+}, which results in a change in the loop conformation bringing the two tryptophan residues closer in proximity. Mas7 and another control, cylicCALP3 (a head to tail cyclic version of CALP3), had no effect on tryptophan emission (Fig. 4*d*). Thus it would appear that as with CaM (see below), CALP2 and -3 are causing changes in TnC that are antagonistic and agonistic, respectively, to the effects of Ca^{2+}. In addition, the effects are due to interactions occurring at or near the EF hands.

NMR Studies of the CALP·CaM Complex—One- and two-dimensional NMR techniques were used to test further for CALP-induced conformational changes in CaM as well as to determine whether the complementary peptides preferentially bind to the Ca^{2+}-coordinating sites in the amino- or carboxyl-terminal domains of CaM. At a 2 to 1 mole ratio of CALP1 to recombinant ^{15}N-labeled *Drosophila* CaM, there are at least 28 new peaks observed in the two-dimensional ^{1}H-^{15}N HSQC spectrum. Of these 28 peaks, 11 overlay with peaks in the Ca^{2+}-bound CaM HSQC spectrum (Fig. 5). The finding that the apoCaM spectra (Fig. 5*a*) is that expected of the Ca^{2+}-free form of the protein would seem to unequivocally demonstrate that the preparation is devoid of Ca^{2+}. Furthermore, the obvious differences between the Ca^{2+} and CALP1 bound CaM (Fig. 5, *b* and *c*) clearly show that the interaction is with CALP1 as opposed to Ca^{2+} contamination of the peptide. Collectively, these results suggest that CALP1 causes conformational changes that in part overlap and yet in other ways are different than those elicited by Ca^{2+}. This idea is confirmed by the

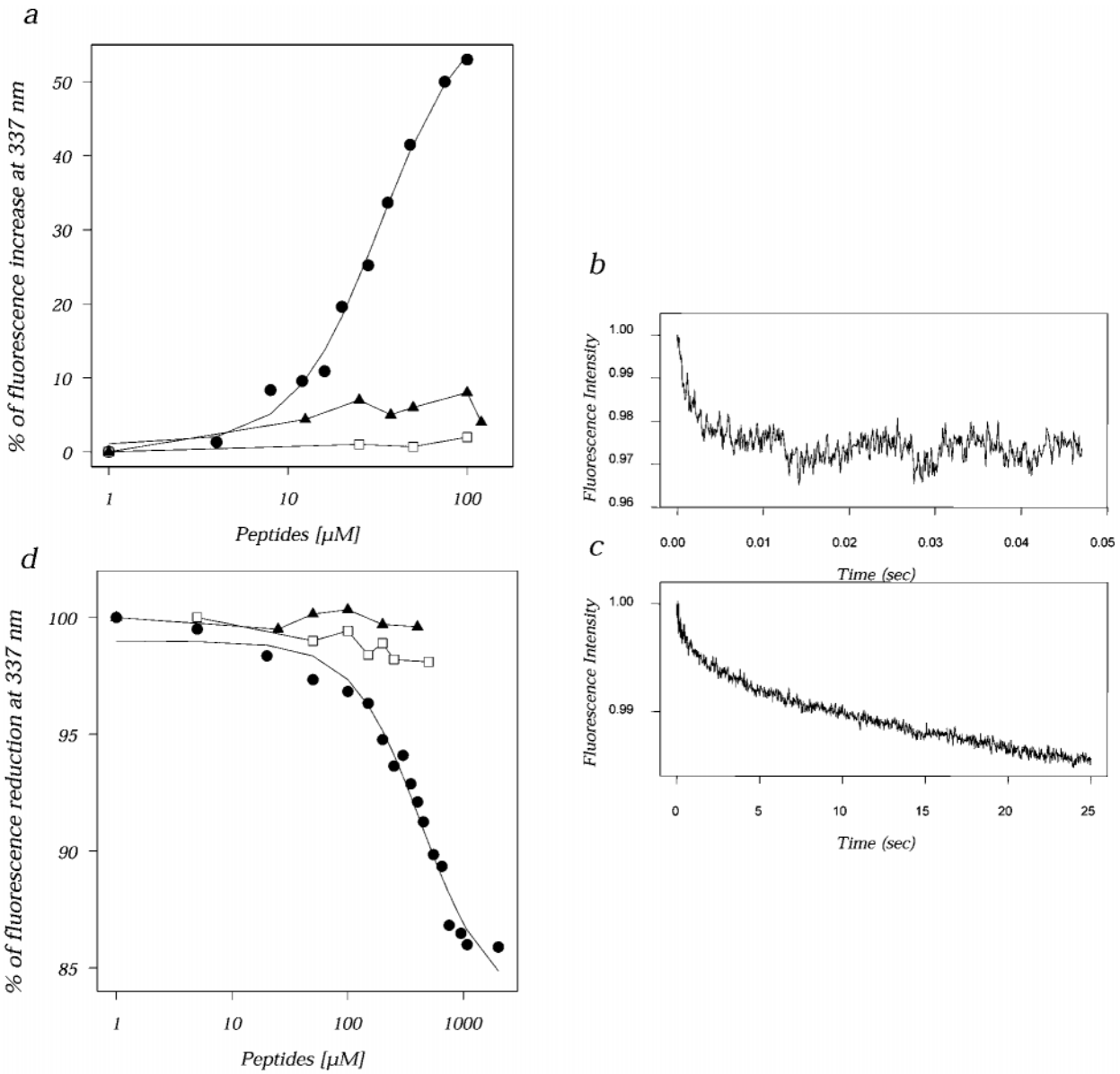

FIG. 4. **Fluorescence studies on the interaction of TnC with CALP peptides.** *a,* changes in maximal emission of smooth muscle C84S/Y111W/R147W TnC (1 μM) induced by CALP2 (●) and control peptides (Scrambled CALP2 (□) and Mas7 (▲)). Data are reported as the percentage of fluorescence emission at 337 nm induced by the peptide relative to the emission in the absence of peptide. *b* and *c*, stop flow analysis of changes in fluorescence emission induced by Ca^{2+} on C84S/R147W TnC in the absence (*b*) or presence (*c*) of CALP2 (75 μM). Note the different time scales. *d*, changes in maximal emission of C84S/Y111W/R147W TnC induced by CALP3 (●) and control peptides (cyclic CALP3 (□) and Mas7 (▲)). Data are reported as the percentage of fluorescence emission at 347 nm induced by the peptide relative to the emission in the absence of peptide.

TABLE II
Fluorescence parameter of TnC and CALP2/TnC complex

Where is λ_{em} = emission maximum with an excitation of 295 nm, K_{SV} is the Stern-Volmer dynamic quenching constant calculated from the acrylamide quenching experiments. The dynamic bimolecular quenching constant (k_q) was calculated from $k_q = K_{SV}/\langle\tau\rangle$, where $\langle\tau\rangle$ is the intensity-weighted mean fluorescence lifetime calculated from $\langle\tau\rangle = \Sigma\,\alpha_i(\tau_i)^2/\Sigma(\alpha_i\tau_i)$.

	λ_{em}	K_{SV}	$\langle\tau\rangle$	$k_q \times 10^{-9}$
	nm	M^{-1}	*ns*	$M^{-1}\ s^{-1}$
TnC	347	18.49	3.93	4.70
CALP2 · TnC complex	337	9.19	4.51	2.03

observation that the majority of the new peaks for CALP1/CaM in common with Ca^{2+}-bound CaM correspond to peaks that are assigned to the carboxyl-terminal domain of CaM. Similar results were obtained with bovine CaM and CALP1, as well as *Drosophila* or bovine CaM and CALP3 (data not shown).

To confirm the possibility that CALP1 and -3 preferentially interact with the carboxyl-terminal region of CaM, the protein was fragmented with trypsin into its amino- and carboxyl-terminal domains. For the amino-terminal domain of apoCaM, there was no evidence by NMR of an interaction with either CALP1 (Fig. 6) or CALP3 (data not shown). In contrast, when the carboxyl-terminal fragments of apo-*Drosophila* (Fig. 7) and bovine (data not shown), CaMs were titrated with CALP1; new peaks arise in the aromatic and methyl regions of the one-dimensional ^1H NMR spectrum (Fig. 7). These peaks show excellent correspondence with peaks that are seen in the Ca^{2+}-bound form of this fragment. Virtually identical results were seen when the carboxyl-terminal fragment of *Drosophila* apoCaM was titrated with CALP3 (data not shown).

The fact that CALP1 and -3 cause Ca^{2+}-like changes in the NMR spectra of the carboxyl- but not amino-terminal fragment of CaM clearly shows that Ca^{2+} contamination is not respon-

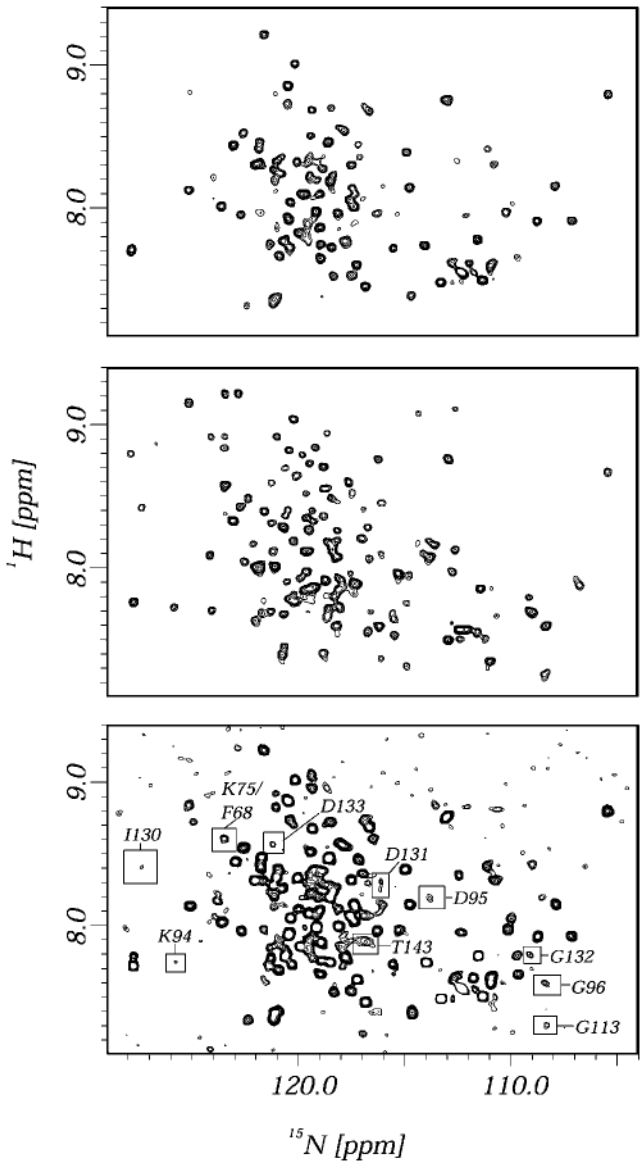

FIG. 5. **Two-dimensional ^{1}H-^{15}N HSQC spectra of ^{15}N *Drosophila* CaM.** *a,* shows the apo-*Drosophila* CaM spectrum. The sample is 0.25 mM CaM, pH 6.3, KCl- and Ca^{2+}-free in 90% H_2O, 10% D_2O. *b,* shows the calcium-bound CaM spectrum, pH 6.3, and KCl-free. *c,* shows the sample from *a* with 1.0 mM CALP1 peptide added. The *boxed peaks* in *c* indicate new peaks that are at the same chemical shift as peaks in the carboxyl-terminal region of calcium-bound CaM. Spectra were acquired on a Bruker AM600 NMR spectrometer and processed with Felix 95.0.

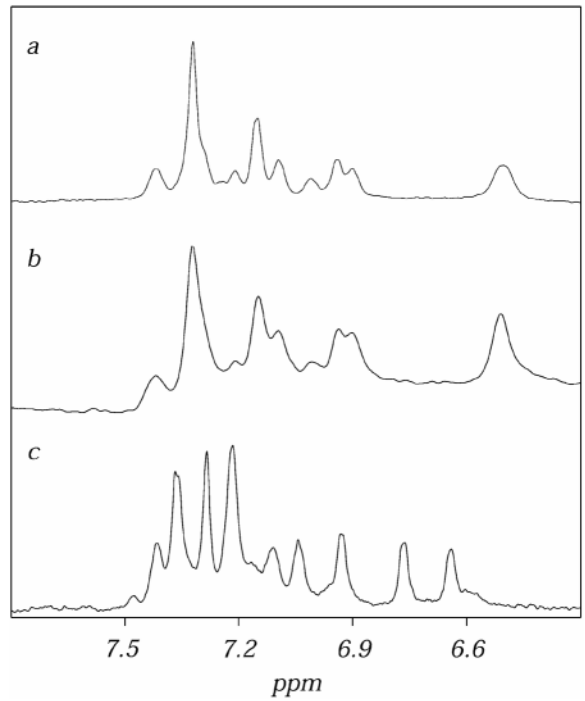

FIG. 6. **Titration of the apo-amino-terminal domain of *Drosophila* CaM with CALP1.** *a* shows the aromatic region of the ^{1}H NMR spectrum of (0.18 mM) apo-amino-terminal CaM domain, pH 7.0, in Ca^{2+}-free 100% D_2O. *b* shows the spectrum from the same sample with 1.0 mM CALP1 peptide added, pH 7.0. *c,* shows the spectrum of the same apo-amino-terminal CaM domain with 2 mM $CaCl_2$ (100% D_2O). Spectra were acquired on a Bruker AM600 NMR spectrometer, using presaturation of the residual HDO. No new or shifted peaks were seen in either the aromatic region or the methyl region of the spectra.

sible for the effects since Ca^{2+} would alter the spectra of both domains. Despite this, two other methods were used to rule out Ca^{2+} contamination. First, a sample of the carboxyl-terminal CaM fragment was prepared in D_2O, and a one-dimensional ^{1}H spectrum was acquired. One-dimensional spectra were then acquired on this sample 24 and 72 h later. Over this period, no change was seen in the spectra indicating that there was not a problem of Ca^{2+} leaching from the NMR tube. There was also no slow conformational change in the free carboxyl-terminal fragment during this period. These results are significant as all CALP/CaM experiments were completed within 24 h. Second, EGTA (5 mM) addition reversed the spectral changes due to Ca^{2+} but not CALP (data not shown).

Collectively, the NMR results confirm and extend those with dansylated CaM. They clearly show that CALP1 and -3 interact with CaM and cause a conformational change. The binding and conformational change, while Ca^{2+}-like, is not identical to that seen with Ca^{2+} since binding preferentially seems to occur in the carboxyl-terminal domain, and the CALP·CaM complexes have peaks in common with, as well as distinct from, those seen in the Ca^{2+}-bound form of CaM.

Activation of Phosphodiesterase (PDE)—The observations that the CALP peptides bind the carboxyl-terminal EF hands of CaM and cause a conformational change raised the question of whether the CALP·CaM complex is in an active or "productive" conformation. This was explored with a Ca^{2+}/CaM-dependent PDE assay employing a fluorescent form of cGMP as the substrate (57, 58). At saturating levels of substrate and low levels of CaM, changes in Ca^{2+} concentration are reflected as a change in the V_{max} of the enzymatic reaction due to the stimulating effect of the active Ca^{2+}-bound form of CaM. By using an EGTA concentration that reduces PDE activity to its basal level (the enzyme activity in the absence of CaM), it was possible to titrate the Ca^{2+} activation of CaM. As had been observed before in a different type of PDE assay (38), CALP1 in the presence, but not the absence, of CaM was able to increase PDE activity (Fig. 8). In contrast, CALP2 and -4 were without effect (Fig. 8). Under the assay conditions (0.1 mM EGTA), any Ca^{2+} contamination of the CALP peptides (see "Experimental Procedures") at the highest peptide dose would have led to only 2.5 nM free Ca^{2+} which is far below that required to activate PDE (Fig. 8).

To determine whether CALP2 and -4 acted as CaM antagonists rather than agonists, PDE activity was measured in the presence of fixed concentrations of Ca^{2+} and CaM and increasing concentrations of the complementary peptides. Both CALP2 and -4 inhibited the Ca^{2+}/CaM-dependent PDE activity (Fig. 9). Since Mastoporan 7 causes a similar effect (Fig. 9), it was not possible in this experimental design to attribute con-

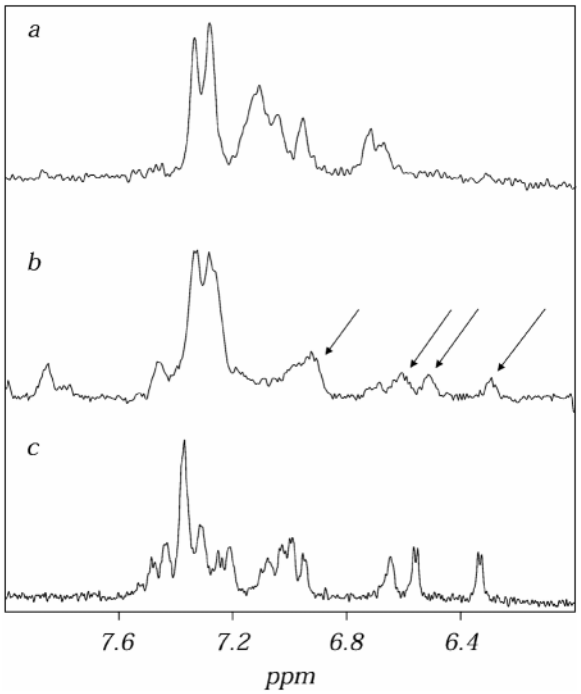

FIG. 7. **Titration of the apo- carboxyl-terminal domain of *Drosophila* CaM with CALP1.** *a* shows the aromatic region of the 600 MHZ ^{1}H NMR spectrum of apo-carboxyl-terminal domain of *Drosophila* CaM. The spectrum was acquired on a 0.12 mM protein sample in 100% D_2O, pH 7.0. *b* shows the spectrum of the same sample with added (1.0 mM) CALP1 peptide. *c* shows the spectrum of the same apo-carboxyl-terminal *Drosophila* CaM with 2.0 mM $CaCl_2$ added. The *arrows* indicate new peaks that arise as CALP1 is added to the protein sample. Similarly, there are also new or shifted peaks in the methyl region of the spectrum of the sample containing CALP1 and of the sample containing calcium.

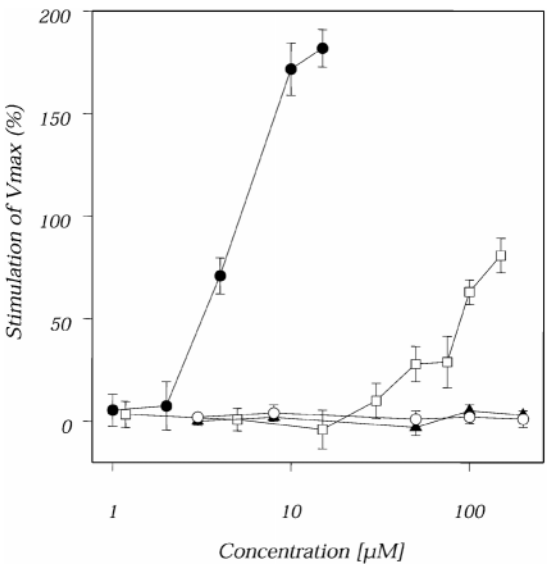

FIG. 8. **Ca^{2+} and CALP1 stimulation of CaM-dependent PDE activity.** The relative activity of PDE in the presence of different concentrations of free Ca^{2+} (●), CALP1 (□), CALP2 (▲), and CALP4 (○) was measured as the slope (absolute value) of the fluorescence change within 5 min of PDE addition. The other reagents were 5 nM CaM, 8 μM Mant-cGMP, 0.1 mM EGTA, and 0.05 units/ml PDE in all of the experiments.

clusively the inhibition of these two peptides to competition for the Ca^{2+}-binding sites as opposed to the PDE-binding site of CaM.

To seek experimental evidence that the mechanism of inhibition of CALP2 was different from that of Mastoporan 7, we

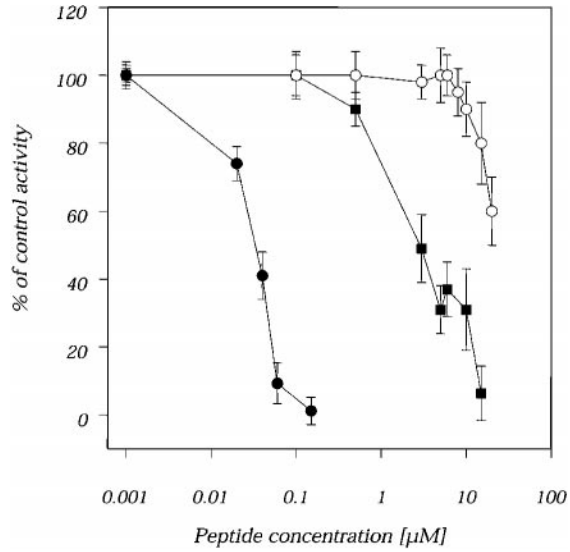

FIG. 9. **CALP2 and CALP4 inhibition of CaM-dependent PDE activity.** CALP2 (■), CALP4 (○), and Mas7 (●) inhibit PDE activity in the presence of Ca^{2+}. The experiment was conducted as for Fig. 8, except for the presence of 5 μM Ca^{2+}. Data are presented as $(V_{max[peptide]}/V_{max(O)}) \times 100$.

investigated the ability of Ca^{2+} to reverse this inhibition. Mastoporan 7 inhibition, based on the binding of the peptide in the hydrophobic core of CaM, cannot be reversed by increasing Ca^{2+} since it requires the divalent cation to bind CaM (Fig. 10). The inhibition due to CALP2, however, could be reversed by Ca^{2+}. This provides strong experimental support for CALP peptides not binding CaM in the hydrophobic core but rather interfering with the calcium-binding site. Additional evidence of the difference between the CALP peptides and peptides binding the hydrophobic core of CaM comes from the analysis of the CD spectra of the CALP peptides. CALP2 and -4 CD spectra are characterized by a negative minimum at 230 nm and by a strong positive maximum between 220 and 200. This is characteristic of a β-sheet or β-turn structure (59). In contrast, other peptides interacting with the CaM hydrophobic core are characterized by an amphiphatic α-helix structure, as is the case for Mas7.

DISCUSSION

One of the major challenges for biological chemistry is to rationally design molecules to interact specifically with given sites of interest on biologically important proteins. The evolving recognition of the role of patterning of hydropathy in protein folding and shape suggested a means to design proteins or peptides with complementary contours by merely inverting hydropathic codes (1). This study reports evidence that *de novo* design by reciprocal patterning of hydropathy can be used to target specifically a peptide to a predetermined site on a protein. In this particular instance, complementary peptides, generically referred to as CALP, were designed with EF hand motifs as the anticipated sites of interaction. The following data are entirely consistent with CALP binding with the expected target on CaM. First, there is a direct interaction measured in real time between CALP and CaM, and this occurs at the Stains-all-binding sites that are known to be EF hands. Second, CALP bound to the EF hands of TnC which precludes an interaction with a hydrophobic core such as that found in CaM. Third, conformational changes like those induced by Ca^{2+} interacting with its coordinating sites are observed in the CALP·CAM complex by NMR spectroscopy as well as by the use of dansylated CaM. Fourth, the conformation of the CALP·CAM complex, like the Ca^{2+}·CAM complex, is compati-

ble with a PDE interaction leading to activation of the enzyme. Throughout these studies, constant attention was taken to ensure that the observed effects were not due to Ca^{2+} contamination. For instance, any Ca^{2+} contamination would have been below the limits of detection by atomic mass spectroscopy and consequently below the amounts required to affect any of the assays. In addition, unlike CALP, which only affected the carboxyl-terminal domain, contaminating Ca^{2+} would have affected the NMR spectra of the amino-terminal as well as carboxyl-terminal fragments of CaM. Finally, EGTA was able to reverse spectral changes in CaM induced by Ca^{2+} but not CALP. Thus it is extremely unlikely that the effects are due to Ca^{2+} contamination.

Although these peptides are termed CALP to indicate Ca^{2+}-like effects or antagonism, NMR determination of a solution structure for CALP1[4] coupled with computer-assisted docking to a known CaM structure (EF hand 4 region) suggest, not unexpectedly, that the interaction with CaM is unlike that of Ca^{2+} (Fig. 11). CALP1 has a complementary contour to a large part of EF hand 4, and only the positively charged amino group on the amino-terminal valine protrudes into the Ca^{2+}-binding pocket. Despite the different binding modalities and obviously different structure, Ca^{2+} and CALP1 interactions lead to similar biochemical and biological effects. There are, of course, examples of similar situations wherein different substances can elicit similar effects by interaction with the same site on a given protein. These include morphine and β-endorphin binding to opiate receptors, acetylcholine and snake neurotoxins interaction with the acetylcholine receptor, and thaumatin and monellin as well as sucrose detection by "sweet" taste receptors (60–62).

In addition to targeting specifically a peptide to a given site on a protein, the feasibility of improving the affinity of interaction as well as changing functional activity was also demonstrated. Two factors that markedly governed affinity were an optimization of reciprocity of the pattern of hydropathy and an increase in peptide length. Interestingly when the two were combined into a single construct, there was an exponential increase in affinity. Increasing the length by four amino acids also changed a given peptide from an agonist for CaM activation of PDE to an antagonist and caused opposing effect on the EF hands of TnC. Although conclusive proof must await the determination of CALP/CAM structures, it is tempting to speculate that the antagonist action occurs as a result of the longer peptides extending out of the Ca^{2+}-binding pockets in CaM. In particular, the three residues of the EF hand loops in CaM are involved in an anti-parallel β-sheet structure between two adjacent Ca^{2+}-binding loops of CaM (44, 45, 53, 57, 58, 63, 64). An interaction of the four amino acid extension with this area of

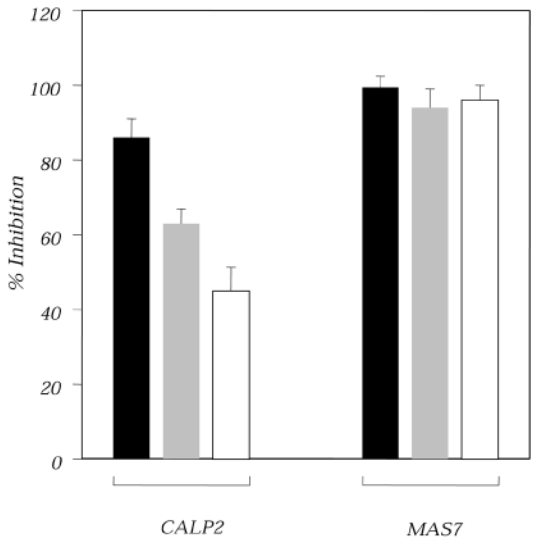

FIG. 10. **Effects of calcium on the inhibition of CaM-dependent PDE activity.** Both CALP2 (15 μM) and Mas7 (0.15 μM) inhibited CaM-dependent activity elicited by 50 μM Ca^{2+} (*black bars*). Mas7 inhibition was not reversed by increasing the calcium concentration to 1 mM (*gray bars*) or 2 mM (*white bars*), whereas CALP2 inhibition was reversed under the same conditions.

[4] M. Villain, P. L. Jackson, M. K. Manion, W.-J. Dong, Z-C. Su, G. Fassina, T. M. Johnson, T. T. Sakai, N. R. Krishna, and J. E. Blalock, manuscript in preparation.

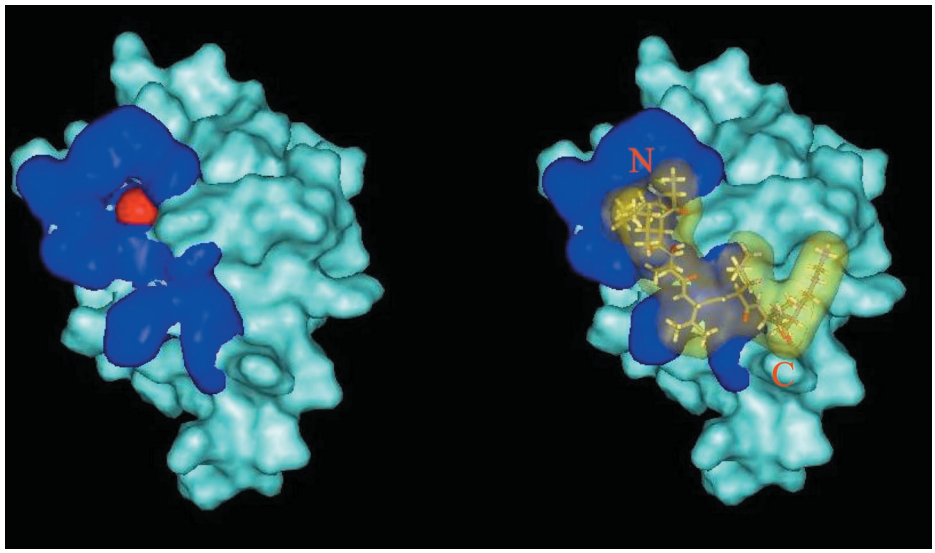

FIG. 11. **Model of CALP1 and CaM.** A possible hypothetical model of interaction between CALP1 and EF loop 4 of calmodulin was obtained using the software Gold (41, 71). The protein structure used was Calmodulin Tr2c-domain (PDB entry 1CMG). The file was elaborated to eliminate the Ca^{2+} atoms, and the amino acids were assigned the theoretical charges at neutral pH using the software Sybyl (Tripos). A surface with a radius of 15 Å centered on tyrosine 99 covering both EF hand 3 and 4 of the model was selected as center of the binding cavity. As ligand we used a model of CALP1 base on NMR data of the peptide in Me_2SO solution. We applied no constraints to the peptide. The model presented is the solution ranked first from the program. On the *left* we present the structure of Tr2C, using a Connolly solvent surface. The *dark blue* area corresponds to EF hand loop IV, and the calcium atom is shown in *red*. The structure on the *right* is the docked model. CALP1 is the transparent *yellow* molecule. Indicated in *red* are the amino terminus and carboxyl terminus of the peptide.

the loop might be expected to interfere with overall conformational changes signaled by alterations in the β-sheet structure.

One unexpected finding in this study was the observation by NMR spectroscopy that CALP interacts with EF hands in the carboxyl-terminal but not the amino-terminal domain. Whereas a molecular understanding of this also awaits three-dimensional structural determinations, interaction in this domain may result from the fact that it contains the two high affinity Ca^{2+}-coordinating sites, and only these may have the requisite structure for CALP binding. Another intriguing question is how an interaction with only one of the two domains leads to a CaM conformation that is capable of activating PDE. This may be related to intermediary conformations of CaM having some enzyme-activating ability (65).

Although this study raises a number of interesting specific questions about CaM, its general conclusion seems clear as follows: hydropathic patterning can be used to tailor-make peptide ligands of varying affinity and opposing (agonist or antagonist) activity that are targeted to predetermined sites on proteins. It would appear that the design principles herein reported may well be generally applicable to other proteins whose classic ligands are not proteinaceous (66). These include "digitalis"-like peptides for the Na^+,K^+-ATPase (67), sapid peptides for taste receptors (68), a "dopamine"-like peptide for the D2 dopamine receptor (69), and an "acetylcholine"-like peptide for the nicotinic acetylcholine receptor (70). We view these peptide ligands as first generation or lead compounds. Once the three-dimensional structure of the peptide ligand-protein target complex is solved, the active conformation of the complementary peptide can then serve as a template for the design of constrained organic analogs with perhaps higher affinities and better pharmacologic profiles.

Acknowledgments—We thank Diane Weigent and Lisa Coplan for expert editorial and technical assistance, respectively.

REFERENCES

1. Blalock, J. E. (1995) *Nat. Med.* **1,** 876–878
2. Clarke, B. L., and Blalock, J. E. (1990) *Proc. Natl. Acad. Sci. U. S. A.* **87,** 9708–9711
3. Weigent, D. A., Clarke, B. L., and Blalock, J. E. (1994) *ImmunoMethods* **5,** 91–97
4. Kamtekar, S., Schiffer, J. M., Xiong, H., Babik, J. M., and Hecht, M. (1993) *Science* **262,** 1680–1685
5. Dill, K. A., Bromberg, S., Yue, K., Fiebig, K. M., Yee, D. P., Thomas, P. D., and Chan, H. S. (1995) *Protein Sci.* **4,** 561–602
6. Riddle, D. S., Santiago, J. V., Bray-Hall, S. T., Doshi, N., Grantcharova, V. P., Yi, Q., and Baker, D. (1997) *Nat. Struct. Biol.* **4,** 805–809
7. Omichinski, J. G., Olson, A. D., Thorgeirsson, S. S., and Fassina, G. (1988) *Protein Society Meeting,* San Diego, CA **321**, (suppl.) 58, The Protein Society, Bethesda
8. Fassina, G., Roller, P. P., Olson, A. D., Thorgeirsson, S. S., and Omichinski, J. G. (1989) *J. Biol. Chem.* **264,** 11252–11257
9. Maier, C. C., Moseley, H. N. B., Zhou, S. R., Whitaker, J. N., and Blalock, J. E. (1994) *ImmunoMethods* **5,** 107–113
10. Blalock, J. E., and Smith, E. M. (1981) *Biochem. Biophys. Res. Commun.* **101,** 472–478
11. Bost, K. L., Smith, E. M., and Blalock, J. E. (1985) *Proc. Natl. Acad. Sci. U. S. A.* **82,** 1372–1375
12. Baranyi, L., Campbell, W., Ohshima, K., Fujimoto, S., Boros, M., and Okada, H. (1995) *Nat. Med.* **1,** 894–901
13. Crawford, S. E., Stellmach, V., Murphy-Ullrich, J. E., Ribeiro, S. M. F., Lawler, J., Hynes, R. O., Boivin, G. P., and Bouck, N. (1998) *Cell* **93,** 1159–1170
14. Ribeiro, S. M. F., Poczatek, M., Schultz-Cherry, S., Villain, M., and Murphy-Ullrich, J. E. (1999) *J. Biol. Chem.* **274,** 13586–13593
15. Ghiso, J., Saball, E., Leoni, J., Rostagno, A., and Frangione, B. (1990) *Proc. Natl. Acad. Sci. U. S. A.* **87,** 1288–1291
16. Palla, E., Bensi, G., Solito, E., Buonamassa, D. T., Gassina, G., Raugei, G., Spano, F., Galeotti, C., Mora, M., Domenighini, M., Rossini, M., Gallo, E., Varinci, V., Bugnoli, M., Bertini, F., Parente, L., and Melli, M. (1993) *J. Biol. Chem.* **268,** 13486–13492
17. Ruiz-Opazo, N., Akimoto, K., and Herrera, V. L. M. (1995) *Nat. Med.* **1,** 1074–1081
18. Smith, L. R., Bost, K. L., and Blalock, J. E. (1987) *J. Immunol.* **138,** 7–9
19. Whitaker, J. N., Sparks, B. E., Walker, D. P., Goodin, R., and Benveniste, E. N. (1989) *J. Neuroimmunol.* **22,** 157–166
20. Zhou, S. R., Han, Q., LaGanke, C. C., and Whitaker, J. N. (1994) *Clin. Immunol. Immunopathol.* **70,** 251–259
21. Zhou, S. R., and Whitaker, J. N. (1994) *ImmunoMethods* **5,** 136–147
22. Zhou, S. R., and Whitaker, J. N. (1993) *J. Immunol.* **150,** 1629–1642
23. Zhou, S. R., Whitaker, J. N., Han, Q., Maier, C., and Blalock, J. E. (1994) *J. Immunol.* **153,** 2340–2351
24. Araga, S., LeBoeuf, R. D., and Blalock, J. E. (1993) *Proc. Natl. Acad. Sci. U. S. A.* **90,** 8747–8751
25. Araga, S., Galin, F. S., Kishimoto, M., Adachi, A., and Blalock, J. E. (1996) *J. Immunol.* **157,** 386–392
26. Boquet, D., Dery, O., Frobert, Y., Grassi, J., and Couraud, J. Y. (1995) *Mol. Immunol.* **32,** 303–308
27. Blalock, J. E., Whitaker, J. N., Benveniste, E. N., and Bost, K. L. (1989) *Methods Enzymol.* **178,** 63–74
28. Déry, O., Frobert, Y., Zerari, F., Créminon, C., Grassi, J., Fischer, J., Conrath, M., and Couraud, J.-Y. (1997) *J. Neuroimmunol.* **76,** 1–9
29. Martins, V. R., Graner, E., Garcia-Abreu, J., deSouza, S. J., Mercadante, A. F., Veiga, S. S., Zanata, S. M., Neto, V. M., and Brentani, R. R. (1997) *Nat. Med.* **3,** 1376–1382
30. McGuigan, J. E. (1994) *ImmunoMethods* **5,** 158–166
31. Jarpe, M. A., and Blalock, J. E. (1994) in *Peptides: Design, Synthesis, and Biological Activity* (Basava, C., and Anantharamiah, G. M., eds) pp. 165–179, Springer-Verlag Inc., New York
32. Blalock, J. E. (1990) *Trends Biotechnol.* **8,** 140–144
33. Borovsky, D., Powell, C. A., Nayar, J. K., Blalock, J. E., and Hayes, T. K. (1994) *FASEB J.* **8,** 350–355
34. Pascual, D. W., and Bost, K. L. (1989) *Pept. Res.* **2,** 207–212
35. Blalock, J. E., and Bost, K. L. (1986) *Biochem. J.* **234,** 679–683
36. Torres, B. A., and Johnson, H. M. (1990) *J. Neuroimmunol.* **27,** 191–199
37. Johnson, H. M., and Torres, B. A. (1994) in *ImmunoMethods* (Langone, J. J., ed) pp. 167–171, Academic Press, Orlando
38. Dillon, J., Woods, W. T., Guarcello, V., LeBoeuf, R. D., and Blalock, J. E. (1991) *Proc. Natl. Acad. Sci. U. S. A.* **88,** 9726–9729
39. Demaille, J. G. (1982) *Calcium Cell Funct.* **2,** 111–144
40. Fassina, G., Cassani, G., and Corti, A. (1992) *Arch. Biochem. Biophys.* **296,** 137–143
41. Jones, G., Willett, P., and Glen, R. C. (1995) *J. Mol. Biol.* **245,** 43–53
42. Dong, W. J., Wang, C. K., Gordon, A. M., and Cheung, H. C. (1997) *Biophys. J.* **72,** 850–857
43. Dong, W. J., Wang, C. K., Gordon, A. M., Rosenfeld, S. S., and Cheung, H. C. (1997) *J. Biol. Chem.* **272,** 19229–19235
44. Andersson, A., Forsen, S., Thulin, E., and Vogel, H. J. (1983) *Biochemistry* **22,** 2309–2313
45. Vogel, H. J., Lindahl, L., and Thulin, E. (1983) *FEBS Lett.* **157,** 241–246
46. Thulin, E., Andersson, A., Drakenberg, T., Forsen, S., and Vogel, H. J. (1970) *Proc. Natl. Acad. Sci. U. S. A.* **71,** 1862–1870
47. Bodenhausen, G., and Ruben, D. J. (1980) *Chem. Phys. Lett.* **69,** 185–189
48. Henikoff, J. G., Henikoff, S., and Pietrokovski, S. (1999) *Nucleic Acids Res.* **27,** 226–228
49. Henikoff, S., and Henikoff, J. G. (1994) *Genomics* **19,** 97–107
50. Caday, C. G., and Steiner, R. F. (1985) *J. Biol. Chem.* **260,** 5985–5990
51. Kincaid, R. L., Vaughan, M., Osborne, J. C., Jr., and Tkachuk, V. A. (1982) *J. Biol. Chem.* **257,** 10638–10643
52. Graff, J. M., Young, T. N., Johnson, J. D., and Blackshear, P. J. (1989) *J. Biol. Chem.* **264,** 21818–21823
53. Vogel, H. J. (1994) *Cell Biol.* **72,** 357–376
54. Kilhoffer, M. C., Kubina, M., Travers, F., and Haiech, J. (1992) *Biochemistry* **34,** 8098–8106
55. Chabbert, M., Lukas, T. J., Watterson, D. M., Axelsen, P. H., and Prendergast, F. G. (1991) *Biochemistry* **30,** 7615–7630
56. Kilhoffer, M. C., Roberts, D. M., Adibi, A. O., Watterson, D. M., and Haiech, J. (1988) *J. Biol. Chem.* **263,** 17023–17029
57. Hiratsuka, T. (1982) *J. Biol. Chem.* **257,** 13354–13358
58. Johnson, J. D., Walters, J. D., and Mills, J. S. (1987) *Anal. Biochem.* **162,** 291–295
59. Woody, W. R. (1985) *The Peptide,* pp. 15–114, Academic Press, San Diego
60. Li, C. H. (1982) in *Biochemical Actions of Hormones* (Litwack, G., ed) pp. 1–41, Academic Press, New York
61. Lentz, T. L., Wilson, R. T., Hawrot, E., and Speicher, D. W. (1984) *Science* **226,** 847–848
62. Ogata, C., Hatada, M., Tomlinson, G., Shin, W. C., and Kim, S. H. (1987) *Nature* **328,** 739–742
63. George, A. J. T., French, R. R., and Glennie, M. J. (1995) *J. Immunol. Methods* **183,** 51–63
64. Browne, J. P., Strom, M., Martin, S. R., and Bayley, M. (1997) *Biochemistry* **36,** 9550–9561
65. Kincaid, R. L., and Vaughan, M. (1986) *Proc. Natl. Acad. Sci. U. S. A.* **83,** 1193–1197
66. Blalock, J. E. (1999) *Cell Mol. Life Sci.* **55,** 513–518
67. Mulchahey, J. J., Nagy, G., and Neill, J. D. (1999) *Cell Mol. Life Sci.* **55,** 653–662
68. Jankov, B. P., Stoineva, I. B., and Petkov, D. D. (1994) *23rd European Peptide Symposium,* European Peptide Society, Braga, p. 324 (abstr.)
69. Nagy, G. M., and Frawley, L. S. (1991) *73rd Annual Endocrine Society Meeting,* The Endocrine Society, Bethesda, p. 209 (abstr. 716)
70. Radding, W., Hageman, G. R., Gantenberg, N. C., Bradley, R. J., Liu, Y., and Kemp, G. (1992) *J. Auton. Nerv. Syst.* **40,** 161–170
71. Jones, G., Willett, P., Glen, R. C., Leach, A. R., and Taylor, R. (1997) *J. Mol. Biol.* **267,** 727–748